Calculating and Measuring the Effects of Polarization Smoothing on Scattering Instabilities in a NIF-like Plasma

J. D. Moody

R. L. Berger

J. E. Rothenberg

Introduction

The present schemes for inertial-confinement-fusion (ICF) target ignition require a high uniformity in the intense laser beams that will strike the target directly (direct drive) or the hohlraum wall (indirect drive).[1] The large-aperture glass laser systems used in ICF applications produce beams with nonuniform intensity speckle structures ("hot spots") at their focus. With intensities that are significantly above the spatial average beam intensity, these hot spots can lead to substantial power losses from stimulated Raman scattering (SRS) and stimulated Brillouin scattering (SBS) in hohlraum plasmas. To reduce these scattering losses, various beam-smoothing techniques have been developed to create more uniform beam intensity distributions.[2–11]

As part of a plan for attaining ignition at the National Ignition Facility (NIF), we used the Nova laser system to systematically study the effectiveness of the beam-smoothing techniques in reducing the backscattered light. Previously, experiments examined the effects of random phase plates (RPPs),[3] kinoform phase plates (KPPs),[10] and smoothing by spectral dispersion (SSD)[4] using a 3-GHz modulator.[11] Under various laser and plasma conditions, these techniques all showed certain advantages with respect to reducing the backscattered light level.

Most recently, we studied the effect of polarization smoothing (PS)[6–9] by itself and combined with smoothing by spectral dispersion, using a high-frequency (17-GHz) modulator. The higher frequency modulator reduces the beam dispersion necessary for optimal SSD, thereby allowing laser propagation through spatial-filter pinholes and hohlraum entrance holes without clipping.[12] This article describes the predicted and measured effects of polarization smoothing (with and without smoothing by spectral dispersion) on the stimulated Raman and Brillouin backscattering. Both the experimental work and the modeling show that the combination of polarization smoothing with smoothing by spectral dispersion gives the greatest reduction in the backscattering levels for SRS and SBS.

Relevance to NIF

Target designs for the NIF currently consist of gas-filled, 9-mm long, Au hohlraums that will be heated with a 1.3-MJ (430-TW peak power) laser, at a 351-nm wavelength.[13] The laser energy will be delivered to the hohlraum by 192 beams in shaped pulses about 20 ns long. The beams will be focused with $f/20$ lenses arranged in clusters of four, effectively producing an $f/8$ beam. For symmetric capsule implosions, two rings each of inner and outer beams will be used, which reach the hohlraum wall at different distances from the laser entrance holes (LEHs) and have different path lengths in the hohlraum plasma.

Beam smoothing will be done by using spectral dispersion with a kinoform phase plate. This phase plate will produce a flat-top focal spot with a factor-of-two intensity variation over the 3- to 5-mm-long laser path in the hohlraum. The point design ignition target[13] is a 300-eV radiation temperature hohlraum, which will contain a low-Z, fully ionized plasma (initially a mix of He and H_2) at about 10% of the critical density. At the time of maximum laser power, the peak laser intensity will be 2×10^{15} W/cm^2 at the best focus of the $f/8$ cluster; other regions along the beam path will have intensities ranging from 10^{15} to 2×10^{15} W/cm^2. Over most of their path lengths, the laser beams will interact with the low-Z plasma. However, for the last 400 μm, the interaction will be with a high-Z, high-T_e Au plasma ablated from the hohlraum wall. The low-Z plasma between the hohlraum wall and the laser entrance holes will have an electron temperature T_e ranging from 3- to 6-keV, and an electron density n_e of from 0.07 n_c to 0.12 n_c ($n_c = 9 \times 10^{21}$/cm^3 for 351-nm light).

We have done calculations and experiments studying the effects of smoothing by spectral dispersion and polarization smoothing in various combinations—with plasma conditions and at length scales that are relevant to NIF. The two NIF plasma conditions that are important to emulate are (1) a long-scale-length (2-mm), low-Z plasma (with a high-gain exponent for stimulated Brillouin and Raman scattering) that the inner-beams encounter and (2) a shorter-scale-length, outer-beam plasma, corresponding to the plasma conditions near the Au wall[14] (with a higher-gain exponent for stimulated Brillouin scattering).
We modeled the low-Z, inner-beam case experimentally with gasbag targets. The NIF's outer-beam plasma was modeled with a scale-1 hohlraum described in a separate article.[15]

Polarization Smoothing: Optical Theory and Experimental Implementation on Nova

Spatial smoothing using a random phase plate works by eliminating the long coherence length in a beam's near field, thereby randomizing and reducing the high-intensity, small-scale structure within the focal spot. A similar kind of spatial smoothing uses a kinoform phase plate, which produces a speckle distribution of intensities in the far field—as does the random phase plate—but which makes the average intensity at focus spatially flat. Smoothing by spectral dispersion causes the local speckle intensity (produced by either type of phase plate) to vary in time at a given spatial location. The laser light is first broadened in frequency by $\Delta\nu$ using frequency modulation (FM) and then it is dispersed with a grating. At any time, the resulting speckle pattern is a superposition of interfering patterns from each wavelength, which decorrelate and yield a new speckle pattern with a coherence time of $\sim 1/\Delta\nu$. Practical limitations in the available laser bandwidth will typically limit the coherence time to a few picoseconds. This is a short enough time to possibly affect the filamentation instability. However, since the scattering instabilities in ICF plasmas typically develop in less than a picosecond, it is also desirable to employ a technique that can smooth out intensity non-uniformities instantaneously. Polarization smoothing provides a way of doing just this.

In polarization smoothing, the near field of the incident laser light is divided into two orthogonal polarizations, each containing half of the beam's incident power. By passing these beams through a phase plate, two uncorrelated speckle patterns are produced, with each beam generating a distinct speckle pattern in the focal plane. One technique used for polarization smoothing is to alternately rotate the polarization by 90° in subapertures of the near-field beam.[7,8] The technique that we chose for Nova uses a birefringent wedge to create orthogonally polarized beams in the same subaperture of the near-field beam.[6] The wedge creates a spatial offset in the speckle patterns corresponding to the two polarizations. In either technique, the speckle intensities in the two beams add incoherently, thus reducing the maximum intensities arriving at the focal plane. The essential advantage of polarization smoothing is that the light intensity is smoothed instantaneously, whereas smoothing by spectral dispersion requires a smoothing time that is inversely proportional to the laser bandwidth.

In polarization smoothing by a wedge, the primary adjustable parameter is the size of the shift generated between the orthogonal speckle patterns. Recent calculations have shown that supression of filamentation is fully effective when PS is used with a minimum shift of one to two speckle half-widths.[9] Since plasma filamentation and stimulated scattering instabilities are generally very sensitive to the transverse scale length of the incident illumination, it is useful to consider the spatial spectrum of the focal-spot intensity pattern resulting from the polarization smoothing of simple square-aperture beams. (Although the spectrum changes slightly in going from square to circular apertures, the qualitative features remain the same.)

The effect of the polarization-smoothing shift on the intensity distribution in the focal plane is best understood in terms of its effect on the spatial spectrum of the speckle intensity. We begin by writing down the spatial power spectral density of the speckle intensity from a uniformly illuminated (but randomly phased) square aperture as:[16]

$$\frac{\left|\tilde{I}(f_x, f_y)\right|^2}{\bar{I}^2} = \Lambda(f_x / f_{\max})\Lambda(f_y / f_{\max}) \Big/ f_{\max}^2 + \delta(f_x, f_y)\,. \quad (1)$$

In this expression, $f_x(k_x/2\pi)$ and $f_y(k_y/2\pi)$ are spatial frequencies of the speckle in the far field, $\Lambda(x) \equiv 1 - |x|$ for $|x| \le 1$, and 0 for $|x| > 1$, $f_{\max} \equiv D / F\lambda$ (where F is the focal length of the lens and D is the aperture width), $\tilde{I}(f_x, f_y)$ is the Fourier transform of the speckle intensity in the far field $I(x_{FF}, y_{FF})$, and $\bar{I} \equiv \left\langle I\left(x_{FF}, y_{FF}\right)\right\rangle$ denotes the average speckle intensity. The first term on the right of Eq. (1) corresponds to the speckle noise and is referred to as the AC spatial-power spectrum; the delta function is determined by the average intensity level.

The spatial power spectrum of the far-field intensity pattern for the two spatially offset speckle patterns, created by the birefringent wedge, can now be quantified. Let the speckle pattern from a single polarization be given by $I_1(x_{FF}, y_{FF})$. Assuming that the wedge disperses the two polarizations by an angle $\Delta\theta$ along the x direction, its effect is to generate two such patterns shifted along x by the distance $\Delta x_{FF} = \Delta\theta F$. Because

there is no interference between the orthogonal polarizations, the total intensity on the target can be written as the incoherent sum

$$I_{\text{total}}(x_{\text{FF}}, y_{\text{FF}}) = I_1(x_{\text{FF}}, y_{\text{FF}}) + I_1(x_{\text{FF}} + \Delta x_{\text{FF}}, y_{\text{FF}}) = I_1(x_{\text{FF}}, y_{\text{FF}}) * \left[\delta(x_{\text{FF}}) + \delta(x_{\text{FF}} - \Delta x_{\text{FF}})\right], \quad (2)$$

where * denotes convolution $\left[a(x) * b(x) \equiv \int a(x-s)b(s)ds\right]$. The Fourier transform can now be taken, to obtain the spatial power spectrum of the total intensity distribution

$$\frac{\left|\tilde{I}_{\text{AC,total}}(f_x, f_y)\right|^2}{\bar{I}_{\text{total}}^2} = 4\left|\tilde{I}_1(f_x, f_y)\right|^2 \cos^2(\pi \Delta x_{\text{FF}} \bullet f_x) / 4\bar{I}_1^2 = \Lambda(f_x)\Lambda(f_y)\cos^2(\pi \Delta x_{\text{FF}} \bullet f_x) / f_{\text{max}}^2 \quad .(3)$$

where the single polarization result of Eq. (1) has been used.

We have now obtained the result that the wedge modifies the spatial spectrum by imposing a sinusoidal modulation, along the shift direction, with a period of $1/\Delta x_{\text{FF}}$. Smoothing very low spatial frequencies requires a large shift, since the first null of the spectral modulation imposed by the polarization smoothing is located at $\pm 1/2\Delta x_{\text{FF}}$. On average, for any shift larger than the speckle half-width $F\lambda/D$, the speckle noise power is reduced by a factor of two; thus, the intensity contrast is reduced by $\sqrt{2}$. This is consistent with simulations of plasma filamentation, which showed that suppression of the instability is fully effective only if the shift is larger than $F\lambda/D$.

The polarization smoothing done in our Nova experiments used a birefringent wedge[6] (a KDP crystal cut at an angle of 41.2° to the optic axis) to create two orthogonally polarized beams with a selected angular deviation (Figure 1). An equal distribution of the incident laser power into each polarization was accomplished by orienting the crystal wedge so that the linearly polarized 351-nm beam (from the frequency-conversion crystals) is incident with its polarization at a 45° angle to the KDP wedge's ordinary (o-wave) and extraordinary (e-wave) axes. The wedge causes the polarizations to be refracted into two beams, separated by an angle, $\Delta\theta = a\Delta n$, where a is the wedge angle and Δn is the birefringence between the ordinary and extraordinary polarizations (0.021 for the KDP used in this experiment).

After passing through the kinoform phase plate (KPP), the two orthogonally polarized beams form identical speckle patterns in the focal plane that are shifted by the amount, $\Delta\theta \cdot F$, where the focal length F is 5.6 m. The minimum shift required to decorrelate a speckle pattern generated by a square near-field beam is the half-speckle width, $F\lambda/D = 3.2$ μm; the incident Nova beam width D was 62 cm.[17] The KDP crystals used for polarization smoothing in our experiments had a wedge angle of 270 μrad. Therefore, they generated an angular shift of 5.7 μrad between the orthogonally polarized beams, which corresponded to about a 30-μm far-field displacement, or about 10 speckle half-widths. This is much larger than the minimum shift of one to two speckle half-widths that was calculated as being required for suppressing filamentation.[9]

In our Nova experiments, we used four subapertures in a 2 × 2 array, similar to the NIF configuration; each subaperture was 27 × 27 cm and was separated by ~8 cm. The half-speckle width from one such subaperture was 7.3 μm; the polarization smoothing shift of 30 μm that resulted is about four times larger than the minimum shift needed to decorrelate the speckle originating from one subaperture. Thus, even for illumination from a single subaperture, filamentation would be effectively suppressed by the 30-μm wedge shift. The direction of the spatial shift from the polarization smoothing was arranged approximately orthogonally to the direction of the shift from SSD. Done in this manner, the polarization smoothing is expected to instantly improve the averaged contrast of the target illumination by a factor of $\sqrt{2}$ beyond that done only with SSD.

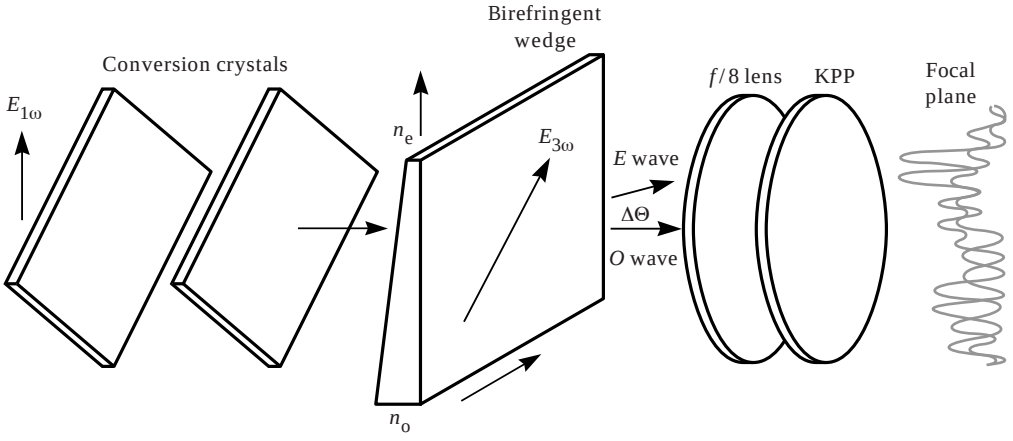

FIGURE 1. Schematic showing the use of a birefringent wedge to generate two shifted and orthogonally polarized speckle patterns for beam smoothing. (08-00-1298-2535pb01)

Polarization smoothing and smoothing by spectral dispersion can be combined to give a more effective smoothing, even though a range of low spatial frequencies is left unsmoothed by this combination. In our experiments, the full extent of the shift obtained with SSD is ~40 μm/Å of bandwidth (specified at the fundamental 1.053-μm wavelength). At a bandwidth of 3 Å, the resulting 120-μm shift is much larger than the 30-μm shift used for polarization smoothing. As a result, if the direction of the latter shift is parallel to the direction of spectral dispersion, little extra benefit might be expected from the added polarization smoothing.

However, because polarization smoothing is instantaneous, it is possible that a significant additional benefit from this method exists for some initial period of time (depending on the response time of the plasma instabilities), even for the case of parallel dispersion directions. This reasoning is supported by simulations of plasma filamentation, which found that SSD and PS dispersions oriented in the same direction work nearly as well at suppressing filamentation as do orthogonally oriented dispersions. However, we did not test this calculation in this set of experiments.[9]

Plasma Theory

The backscattering of laser light begins when a background plasma density fluctuation reflects a small fraction of the incident laser light via Thomson scattering. As the backscattered light interferes constructively with the incoming light, the resulting ponderomotive force enhances the density perturbation. If threshold conditions are satisfied, an instability, resulting in stimulated backscatter, can develop. If the density perturbation is an ion acoustic wave, stimulated Brillouin scattering (SBS) occurs; if the perturbation is a Langmuir wave, stimulated Raman scattering (SRS) occurs.

The laser speckles (hots pots) are also subject to a self-focusing instability (filamentation) in the plasma. This occurs when the light's ponderomotive force and the increased electron pressure (from local laser power absorption) act to expel plasma, thereby increasing the refractive index and further concentrating the light energy into a smaller volume. Smoothing by spectral dispersion reduces this tendency towards filamentation, if the speckle dissolves before the self-focusing process is complete. Thus, it is most effective on lower-intensity hot spots. In addition, polarization smoothing controls filamentation by reducing the fraction of the laser power present in high-intensity speckles. We expect then, that a combination of the two smoothing methods should be very effective for filamentation control.

Because the background density fluctuations tend to be very small, the mean intensity of the backscattered light must grow by about 10 orders of magnitude to scatter a significant portion (such as 10%) of the laser light. In contrast to this, a self-focusing amplification (resulting from filamentation) of as little as 2.7 times is dramatic. This is because, with a typical hot spot having an intensity twice that of the mean intensity, a great deal of laser energy can be transferred to high intensity and subsequently backscattered.

It appears that a bandwidth sufficient to reduce filamentation might also reduce the faster-growing stimulated Brillouin scattering, if the laser hot spot dissolves before the scattered light fully amplifies. The growth rate for stimulated Brillouin scattering exceeds that for filamentation, but is almost an order of magnitude smaller than for stimulated Raman scattering. The latter will grow to saturation in a few picoseconds for laser and plasma parameters that are of interest to ICF, long before smoothing by spectral dispersion can change the speckle pattern. On the other hand, polarization smoothing is instantaneous and it will reduce both stimulated Raman scattering (to the extent that SRS relies on higher-intensity speckles) and the stimulated Brillouin scattering.

The arguments just given for the effect of polarization smoothing considered each instability in isolation. Actually, the stimulated Raman and Brillouin scatterings, and filamentation instabilities, all interact with one another, leading to a complex beam-smoothing response. We used the F3D code[18] to simulate beam-smoothing effects on interacting stimulated Raman and Brillouin scatterings.[19] Filamentation was included in all cases. The plasma parameters that were chosen in the first simulations are representative of the NIF inner beams (n_e/n_c = 0.1; low-Z; combination of C_3H_8 and C_5H_{12}; T_e = 3 keV; $T_i/T_e = 0.15$; 2×10^{15} W/cm^2). The plasma length along the laser propagation direction (L_z = $1000\lambda_0$) is twice the length of the $f/8$ speckle; the plasma width in the x and y transverse directions is $160\lambda_0$. The intensity-gain exponents for the stimulated Raman and Brillouin scatterings are 12 and 9, respectively. These values are about one-half of those calculated for NIF and for the gasbag experiments reported in this article, primarily because of the shorter plasma length used in the simulation. Thus, we are using the simulations as a qualitative guide to the trends in the data. With a transverse resolution of 1.25 λ_0, there are 440 independent phase-plate elements or independent Fourier components for the incident laser light, which is a statistically representative sample.

In Figure 2, we show the stimulated Raman and Brillouin scattering reflectivities for different smoothing conditions, when both stimulated scatterings are competing for laser energy. In this case, smoothing by spectral dispersion would appear to be more effective than polarization smoothing in suppressing the SBS. However, this happens merely because the SRS has taken a significant amount of energy from the

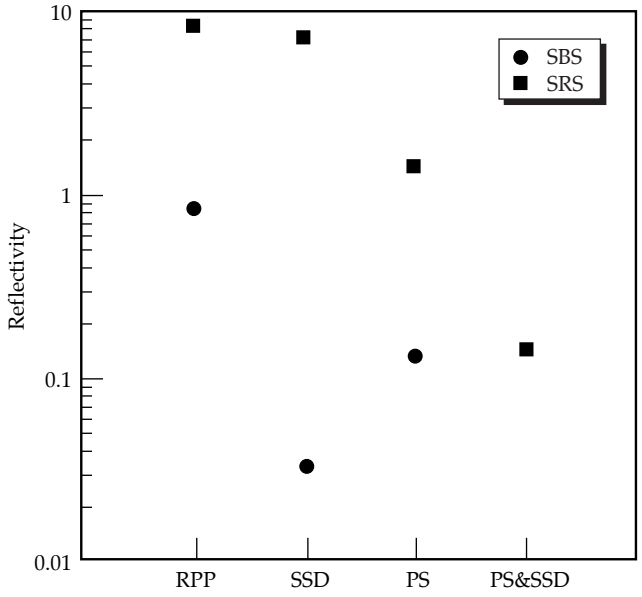

FIGURE 2. The stimulated-Raman-scattering and stimulated-Brillouin-scattering reflectivities, in a 10% critical plasma, are shown for different smoothing conditions when both instabilities are present in the simulation. (08-00-1298-2536pb01)

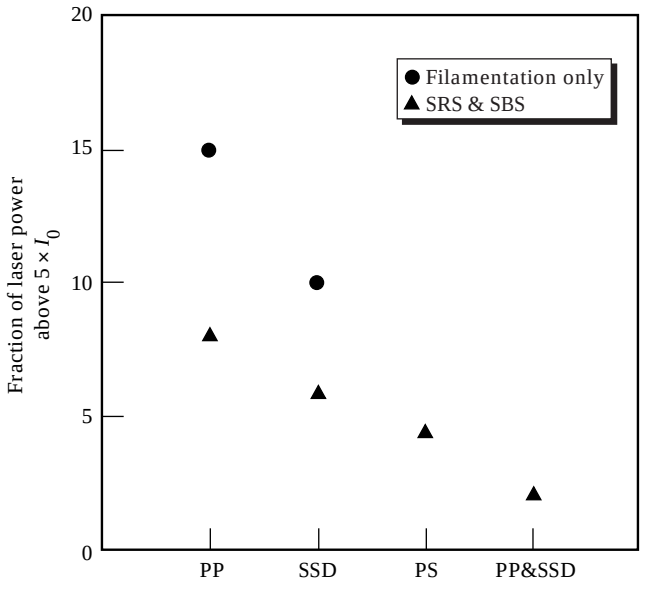

FIGURE 3. The stimulated-Brillouin-scattering reflectivity and the fraction of laser energy having more than five times the average intensity (I_0), for different smoothing conditions. The values have been averaged over the last 20 ps of the simulation to eliminate transient effects ($T_i/T_e = 0.11$; the axial length, $L_z = 351\ \mu m = 1000\lambda_0$; an electron temperature of 2.7 keV; and an electron density of $0.07\ n_c$) (08-00-1298-2537pb01)

high-intensity laser hot spots in the SSD case, which suppresses the SBS. Simulations without SRS show a SBS reflectivity dependence on smoothing that is similar to the SRS dependence shown in Figure 2.

An interesting feature of Figure 2 is the prediction that the combined smoothing techniques will dramatically suppress stimulated Brillouin scattering, as well as reduce stimulated Raman scattering—despite the very fast growth rate of the latter. We attribute this reduction to the effective control of filamentation that the combined techniques have, as is shown in Figure 3. Here, the fraction of laser beam power at an intensity greater than $5 \times I_0$ (where I_0 is the average intensity) is shown as a function of beam smoothing, with and without stimulated backscatter. Without polarization smoothing, the simulations with backscatter show less power at high intensity because power is lost from the speckles as they start to self focus. With polarization smoothing, there is too little backscatter to affect the self-focusing. Combining SSD and PS reduces the power at high intensity more than either method does individually. This fact can explain the simulation result that smoothing by spectral dispersion reduces the stimulated Raman scattering when polarization smoothing is also used.

Using F3D simulations, we have shown that polarization smoothing is a very promising beam-smoothing technique for controlling laser plasma instabilities. This is especially true with respect to stimulated Raman scattering, which the more common smoothing-by-spectral-dispersion technique cannot directly control, because the scattering grows to saturation before the hot spots can be relocated. However, smoothing by spectral dispersion combined with polarization smoothing is particularly powerful. The latter method dramatically reduces the fraction of the beam power at high intensity, thus lowering filamentation growth rates and Brillouin instabilities to a level ($\Delta\omega \approx \gamma_0$) where the smoothing by spectral dispersion is more effective. At these levels, smoothing by spectral dispersion can also indirectly reduce stimulated Raman scattering by reducing self-focusing of the hot spots.

We also carried out simulations with plasma conditions that favored growth of stimulated Brillouin scattering over stimulated Raman scattering ($T_i/T_e = 0.11$; an axial length, $L_z = 351\mu m = 1000\lambda_0$; an electron temperature of 2.7 keV; and an electron density of $0.07 n_c$). Under these conditions, the stimulated Raman scattering is always insignificant, and the stimulated-Brillouin-scattering reflectivity follows similar trends to those shown in Figure 2 for the stimulated-Raman-scattering reflectivity.

Gasbag Plasma Experiments

We used the Nova laser to do experiments with targets developed to reproduce the plasma conditions and length scales of the NIF. As mentioned earlier, the

two plasma conditions of importance for the NIF are the inner-beam plasma (a large-scale-length, low-Z plasma, with high-gain exponents for both stimulated Raman and Brillouin scatterings), and the outer-beam plasma (with shorter scale lengths and a higher-gain exponent for stimulated Brillouin scattering in the plasma near the Au wall).[19]

The low-Z, inner-beam case was studied with gasbag targets. These consist of two membranes, one on either side of a thin Al washer, which are inflated with a C_3H_8 and C_5H_{12} gas mixture at a one atmosphere pressure to produce an almost spherical gas volume. Nearly symmetric irradiation by nine heater beams produces a 6% to 15% critical-density plasma, with 1- to 2-mm scale lengths and a peak central $T_e = 3$ keV. The tenth Nova beam, called the interaction beam, was used to drive the instabilities in the plasma. It was configured as an $f/8.5$ beam, with options for smoothing by spectral dispersion and polarization smoothing.

Figure 4 shows the stimulated Raman and Brillouin scattering reflectivities that were measured from gasbag targets. Most of the data shown is for intensities of ~2×10^{15} W/cm^2. All targets with density above 13% critical used a higher interaction intensity of ~5×10^{15} W/cm^2. These high-intensity experiments were intended to explore the conditions expected in a higher-radiation-temperature, NIF-hohlraum design. Most of the data points show that, while polarization smoothing reduces the scattering levels, the reduction is not as significant as when it is combined with SSD. This combination gave the most effective beam smoothing ever observed in Nova gasbag experiments. These results show that NIF will benefit from polarization smoothing of the inner beams.

Some of the backscatter data taken with gasbag targets show stimulated Raman and Brillouin scattering values with large departures from their respective averages. We have identified possible systematic reasons for these departures in some, but not all, cases. Backscattering values that exhibit a sudden departure from the average are typically characterized by an increase (decrease) in the SRS and a decrease (increase) in the SBS. We are continuing to analyze the full data set in an effort to identify all reasons for scatter in the data. These observations, if borne out by further analysis, indicate that the interdependence of SRS and SBS makes the study of the effect of beam smoothing on one, or both, more complicated. We are continuing our efforts to develop a predictive model for laser beam filamentation and SBS and SRS backscatter (F3D) that will enable us to calculate the interaction of a complete NIF beam with a macroscopic target.

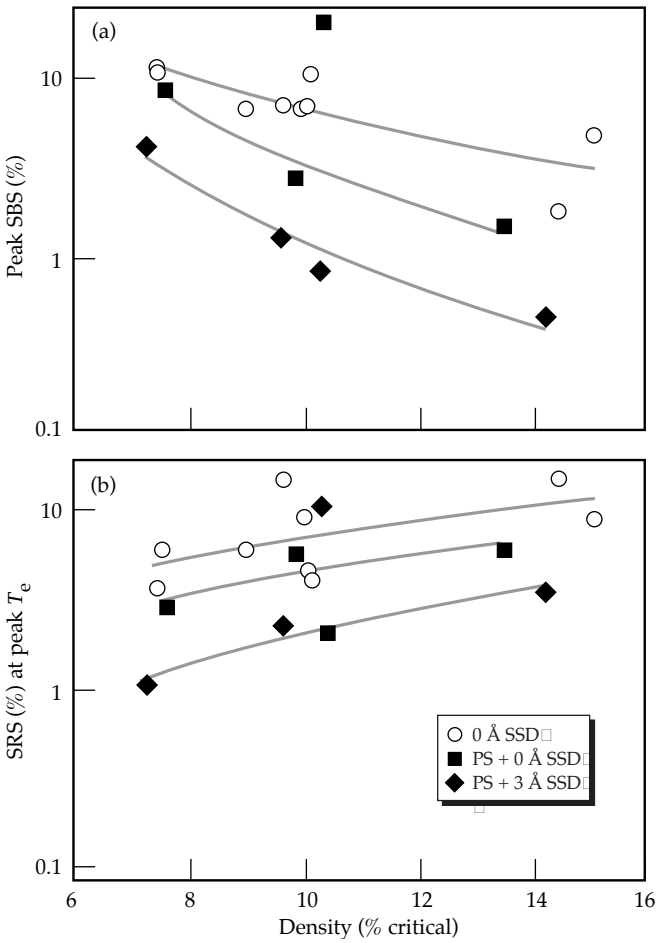

FIGURE 4. Experimental measurements of the (a) stimulated-Brillouin and (b) stimulated-Raman scattered light in gasbag plasmas. The probe intensity is 2×10^{15} W/cm^2, except at the high density where it is 5×10^{15} W/cm^2. The SSD bandwidth is given at 1.053 nm. The scattering includes backscattered light measured in a 15° cone around the backward direction. (08-00-1298-2538pb01)

Conclusions

Our F3D numerical simulations have given us a very optimistic view about the usefulness of polarization smoothing as a highly effective smoothing technique for suppressing laser-plasma instabilities. Although the data indicates that polarization smoothing, by itself, is only partly effective at reducing backscattering losses, our measurements confirm the trends in the simulations. In particular, they show that combining polarization smoothing with smoothing by spectral dispersion provides the most effective way to suppress the instabilities.

The peak scattering observed over the entire experimental range under the maximum (combined) smoothing conditions is below 6% most of the time. Occasionally, either the stimulated Raman or the stimulated Brillouin scattering exhibits a jump, with a corresponding drop in the other, which (in some cases) can be associated with a density or temperature change in the gasbag plasma. Other cases exist, however, in which the sudden jumps in scattering cannot yet be associated with a possible cause. We are continuing to investigate the details of these cases and are

developing a more rigorous connection between the jump in scattering levels and a change in plasma or laser parameters.

The stimulated Brillouin and Raman scatterings in NIF-scale hohlraums should be at tolerable levels with moderate amounts of beam smoothing, even at the higher intensities and densities expected in the 350-eV ignition designs. Our polarization smoothing experiments suggest that this technique, when combined with smoothing by spectral dispersion, can improve the margin against plasma instabilities, thereby increasing the operating region available to the NIF for ICF experiments. The experimental results strongly suggest considering a retrofit of the NIF to include polarization smoothing and its further investigation as part of the experiments scheduled for the NIF's first bundle.

Acknowledgments

The authors acknowledge the contributions of B. J. MacGowan, S. H. Glenzer, R. K. Kirkwood, C. Geddes, L. J. Suter, E. Lefebvre, A. B. Langdon, E. A. Williams, and B. Still.

Notes and References

1. J. D. Lindl, *Phys. Plasmas* **2**, 3933 (1995).
2. R. H. Lehmberg and S. P. Obenschain, *Optics Comm.* **46**, 27 (1983); R. H. Lehmberg and J. Goldhar, *Fusion Technology* **11**, 532–541 (1987).
3. Y. Kato, K. Mima, N. Miyanaga, S. Arinaga, Y. Kitagawa, M. Naktsuka, and C. Yamanka, *Phys. Rev. Lett*. **53**, 1057–1060 (1984).
4. S. Skupsky, R. W. Short, T. Kessler, R. S. Craxton, S. Letzring, and J. M. Soures, *J. Appl. Phys*. **66**, 3456 (1989).
5. J. E. Rothenberg, *Proc. Soc. Photo-Opt. Instrum. Eng*. **2633**, 634 (1995).
6. "Phase Conversion Using Distributed Polarization Rotation," *LLE review* **45**, 1–12 (1990).
7. K. Tsubakimoto, M. Nakatsuka, H. Nakano, T. Kanabe, T. Jitsuno, and S. Nakai, *Opt. Commun*. **91**, 9–12 (1992); K. Tsubakimoto, T. Jitsuno, N. Miyanaga, M. Nakatsuka, T. Kanabe, and S. Nakai, *Opt. Commun*. **103**, 185–188 (1993).
8. S. Pau, S. N. Dixit, and D. Eimerl, *J. Opt. Soc. Am. B* **11**, 1498 (1994).
9. E. Lefebvre, R. L. Berger, A. B. Langdon, B. MacGowan, J. E. Rothenberg, and E. A. Williams, *Phys. Plasmas* **5**, 2701 (1995).
10. S. N. Dixit, J. K. Lawson, K. R. Manes, H. T. Powell, and K. A. Nugent, *Opt. Lett*. **19**, 417 (1994).
11. B. J. MacGowan et al., *Phys. Plasmas* **3**, 2029 (1996). B. J. MacGowan et al., *Proceedings of the IAEA, 16th International Conference on Plasma Physics and Controlled Nuclear Fusion,* Montreal, Quebec, Canada, Oct. 1996, *Fusion Energy* 1996, Vol. 3, 181 (1997).
12. B. J. MacGowan et al., *Proceedings of the IAEA, 17th International Conference on Plasma Physics and Controlled Nuclear Fusion,* Yokohama, Japan, Oct. 1998, *Fusion Energy 1998*, in press. (Article preprint available as: *Laser Beam Smoothing and Backscatter Saturation Processes in Plasmas,* UCRL-JC-132191.)
13. S. W. Haan et al., *Phys Plasmas* **2**, 2480 (1995).
14. Y. Kato et al., *Phys. Rev. Lett*. **53** 1057 (1984).
15. S. H. Glenzer et al., *ICF Quarterly Report*, **8**(1), 7–14, Lawrence Livermore National Laboratory, Livermore, CA, UCRL-LR-105821-98-1 (1997).
16. J. W. Goodman, "Statistical Properties of Laser Speckle Patterns," in *Topics in Applied Physics*, J. C. Dainty, ed., vol. 9, pp. 12–29, Springer-Verlag, New York (1984).
17. *Ibid*, pp. 35–40.
18. R. L. Berger, C. H. Still, E. A. Williams, and A. B. Langdon, manuscript submitted to *Physics of Plasmas* (1998).
19. S. H. Glenzer et al., *Phys. Rev. Lett*. (1998).